SERI/TP-31-118

INTRODUCTION TO LOW ENERGY ION SCATTERING SPECTROSCOPY

H. F. HELBIG
DEPARTMENT OF PHYSICS
CLARKSON COLLEGE OF TECHNOLOGY
POTSDAM, N.Y.

A. W. CZANDERNA
MATERIALS BRANCH, RESEARCH DIVISION
SOLAR ENERGY RESEARCH INSTITUTE

TO BE PUBLISHED AS AN EMMSE
(EDUCATIONAL MODULES FOR MATERIALS
SCIENCE AND ENGINEERING)
TEACHING MODULE.

Solar Energy Research Institute

1536 Cole Boulevard
Golden, Colorado 80401

A Division of Midwest Research Institute

Prepared for the
U.S. Department of Energy
Contract No. EG-77-C-01-4042

SERI/TP-31-118

INTRODUCTION TO LOW ENERGY ION SCATTERING SPECTROSCOPY

H. F. HELBIG
DEPARTMENT OF PHYSICS
CLARKSON COLLEGE OF TECHNOLOGY
POTSDAM, N.Y.

A. W. CZANDERNA
MATERIALS BRANCH, RESEARCH DIVISION
SOLAR ENERGY RESEARCH INSTITUTE

TO BE PUBLISHED AS AN EMMSE
(EDUCATIONAL MODULES FOR MATERIALS
SCIENCE AND ENGINEERING)
TEACHING MODULE.

Solar Energy Research Institute

1536 Cole Boulevard
Golden, Colorado 80401

A Division of Midwest Research Institute

Prepared for the
U.S. Department of Energy
Contract No. EG-77-C-01-4042

TABLE OF CONTENTS

I. OBJECTIVES

After studying this module, the student should be able to:

1. Explain the physical principles underlying the technique of low energy ion scattering spectroscopy.
2. Derive the equation which relates the scattered ion energy to the surface atom mass.
3. Discuss the factors which influence the scattered ion yield.
4. Describe the apparatus required to obtain ion scattering spectra.
5. Interpret simple ion scattering spectra.
6. Distinguish situations for which ion scattering spectroscopy is suitable from those for which it is not.
7. Discuss the strengths and weaknesses of the technique.

II. PREREQUISITES

The students should be familiar with the principles of classical and modern physics, chemistry, and materials science to the level covered in introductory college courses for science and engineering students. Texts commonly used for such courses are:

A. Fundamentals of Physics, Halliday and Resnick, Wiley, N.Y., 1974.
B. Chemical Principles, Masterson and Slowinski, Saunders, N.Y., 1967.
C. Concepts of Modern Physics, Beiser, McGraw - Hill, N.Y.
D. Elements of Materials Science and Engineering, Van Vlack, Addison - Wesley, N.Y., 3rd ed., 1975.

PREREQUISITE QUESTIONS

1. In what type of collision is momentum conserved? In what type of collision is energy conserved? (Ref. A, Chap. 7)

2. Under what conditions does quantum behavior reduce to classical behavior? Review the conditions for the validity of classical behavior and for wave mechanics. (Ref. C)

3. Draw schematically a potential energy curve for an atom in a three-dimensional crystal. Estimate the vibrational amplitude of a copper atom at 300K. Assume it is a simple harmonic oscillator with a frequency of 10^{13} Hz.

4. Show that the addition of vector momenta of $5\hat{\imath}$ (kg-m/s) and $-2\hat{\imath} + 3\hat{\jmath}$(kg-m/s) yields a new vector of $3\hat{\imath} + 3\hat{\jmath}$(kg-m/s). Draw the three vectors. (Ref. A)

5. Review the concept of differential scattering cross-section.

6. A beam of singly charged ions of various energies is directed along the midplane (dotted line) between the two parallel plates (2 cm apart) shown at the bottom of the page.

   (a) Show that the fractional energy spread of the ions that pass through the exit slit (0.1 mm) is about 1%.

   (b) If the plates are 10 cm long and a potential difference of 100 volts exists between them, what is the energy of the ions in part (a)?

Comment: Similar devices, called electrostatic analyzers, are often used to direct ions of selected energy into a detector at the exit slit. Note that such analyzers select for ion energy regardless of the mass of the ion. Note also that energy selection is made by varying the potential between the plates.

Define the following terms:

Potential Energy	Kinetic Energy
Momentum	Electron Volt (eV)
Elastic Scattering	Inelastic Scattering
Isotope	Gaussian Curve
(100), (110) and (111) Planes in a Solid	Electrostatic Analyzer

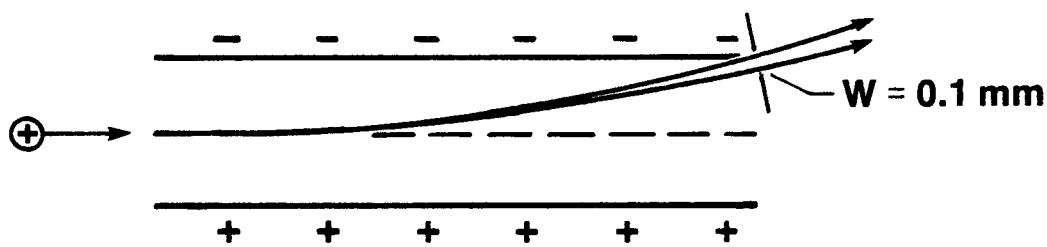

III. INTRODUCTION

The properties of the solid-gas and solid-solid interface phase are studied using a wide variety of experimental methods. An understanding of these phase boundaries is important to many areas of applied science such as catalysis, corrosion, semiconductor devices, adhesion, diffusion, sintering, mechanisms of failure, and energy conversion devices. A realistic view of the boundary is not the obvious, ideal, infinite and uncontaminated plane but a boundary with a variety of more or less imperfect crystal faces varying in composition, structure, and orientation according to the pretreatment of the solid. Residual species may accumulate in the boundary region, drastically altering the behavior of the material.

Parameters of major importance for characterizing the gas-solid interface are surface area, pretreatment, chemical composition, structure, adsorbed species (amount, locations, and interactions), topography, and depth of the surface phase. Ion scattering spectroscopy (ISS) can identify the exposed atoms that form the surface monolayer, can provide at least semiquantitative measures of the relative concentrations of the identified surface atoms and, by ion-etching, can provide the same information about subsurface regions including solid-solid interfaces.

Because of the importance of surface composition in the technology of surfaces, a large number of probes have been developed to determine the elemental composition of a surface. This module considers only positive ions as the surface probe and detection of the scattered ions with the primary goal of determining the elemental composition of the surface.

As shown in Figure 1, ions impinging on a solid may produce particles, ions, electrons, photons, and neutral atoms and molecules. Detection of the particles may be concerned with the kind of particle (mass and charge), their number, energy, and spatial distribution. It is necessary to correlate the detected information with the elements present on the surface.

At the energies (1-2 keV) and incident angles ($0°$-$45°$ from the surface normal) typically used in ISS, most of the probe ions penetrate deeply into the solid with only small deflec-

tions until their energy is reduced, primarily through interactions with electrons of the solid, to thermal levels. They become trapped or diffused among the atoms of the solid. A small fraction of the incident ions, however, will undergo one or more collisions in such a way that they escape the surface (backscatter) with varying amounts of their original energy. Whether implanted or backscattered, they may cause atoms at or near the surface to be ejected (sputtered). Most of the scattered particles are neutralized during their encounter with the solid, but those which retain their electric charge are analyzed according to their energy to form the spectra used in ISS. (In another technique called Secondary Ion Mass Spectroscopy, SIMS, the sputtered surface ions are identified by mass spectroscopy). For ISS, analysis of the scattered primary ions does not require removal of surface atoms, but in fact prolonged bombardment will cause erosion of the surface by sputtering.

In addition to the detection of scattered and sputtered ions, other information about the surface can be obtained by analyzing neutral particles, secondary electrons, and photons as indicated in Figure 1. Techniques utilizing the detection of these output particles have been investigated but have not yet led to commercially available instruments. Instruments for ISS (and SIMS), on the other hand, are currently available from several manufacturers. Discussion of alternative surface analysis techniques can be found in the references mentioned under Further Reading.

The remainder of the module concerns the principles, instrumentation, and information obtainable from ISS. The effects of ion implantation resulting from ion bombardment and the complexities of ion-etching (milling), which must be considered when obtaining composition versus depth information, are important related subjects but are beyond the scope of this module.

IV. PHYSICAL PRINCIPLES

A. Introduction

In ISS a collimated beam of singly charged noble gas ions (e.g. helium, neon, or argon) of known mass (M_i) and energy (E_o) is directed toward a solid surface, and the current (I) of ions backscattered from the surface at some fixed angle (θ) is measured as a function of scattered ion energy (E). Curves of I vs. E, which are the ion scattering spectra, contain useful information because the scattered ions result almost entirely from single collisions with surface atoms (see Figure 2). The probability that an ion will strike two or more surface atoms before backscattering is small, and incident ions which penetrate even one atomic layer below the surface before backscattering are (with high probability) neutralized and so do not contribute to the current, I.

Each ion which contributes to I performs work during its single surface collision as the repulsive force which it exerts on its collision partner accelerates that surface atom from rest to some final kinetic energy, E_r. As a result of that exertion, the scattered ion loses energy, E_r, and, as will be shown below, the amount of that energy loss depends on the mass, M_s, of the recoiling surface atom. As a result, scattered ions will appear, with high probability, only at the energy

$$E(M_s) = E_o - E_r(M_s) \qquad \text{(Eq. 1)}$$

If the surface contains atoms of several different masses, the I versus E curve will consist of a series of current peaks at the energies given by Eq. (1) for each surface atom mass. From the indicated energies, the masses of the surface atoms can be calculated. [Did you do Prerequisite Question 1?]

B. Validity of Classical Mechanics

At the energies and scattering angles commonly used for ISS, the wave-like properties of the colliding atoms are unimportant, and the motion of the deflected ions can be analyzed using classical mechanics. For the quantum description of scattering to reduce to the classical description, one condition is that the de Broglie wavelength λ of the incident particle should change slowly during the collision. In other words, λ must be small compared with the distance over which λ changes by an appreciable fraction. Since changes in the potential energy of interaction V are the cause of the change in λ,

an equivalent condition is that the change ΔV in V which occurs in a distance λ, $\Delta V \cong \lambda dV/dr$, must be a small fraction of V;

$$\left|\frac{\Delta V}{V}\right| = \left|\frac{\lambda}{V}\right|\left|\frac{dV}{dr}\right| \ll 1 \qquad \text{(Eq. 2)}$$

To show that this is the case, the Coulomb potential

$$V = Z_1 Z_2/r \qquad \text{(Eq. 3)}$$

may be used to represent the interaction energy. Here, Z_1 and Z_2 are the nuclear charges of the ion and the target atom, respectively. Then

$$|dV/dr| = Z_1 Z_2/r^2 \qquad \text{(Eq. 4)}$$

and Eq. (2) may be written

$$|\Delta V/V| = \lambda/R \qquad \text{(Eq. 5)}$$

where R is the distance where V changes most rapidly. For a particle of momentum p, the de Broglie wavelength is given by

$$\lambda = h/p \qquad \text{(Eq. 6)}$$

where h is Planck's constant. As an example, a 1500 eV $^3He^+$ ion has a de Broglie wavelength of about 4×10^{-13} m. The value R where the potential energy is changing most rapidly is the distance of closest approach of the colliding particles. Quantum mechanical calculations of the forces between atoms show this distance to be about 10^{-12} m for a 1500 eV head-on He - Cu collision. Using these values, the left side of the inequality in Eq. (2) has a value of about 0.4. For heavier ions at the same energy, the conditions for classical mechanics are even more favorable.
[Do Exercise 1].

Because of the uncertainty principle there is, in general, a second condition on the application of classical mechanics to collision problems. Since the incident particle is localized during the collision to within some distance Δy in a direction transverse to its motion, the uncertainty principle

$$\Delta y\, m \Delta v_y \geq h/4\pi \qquad \text{(Eq. 7)}$$

shows that there must be a corresponding uncertainty Δv_y in the transverse velocity v_y:

$$\Delta v_y \geq h/4\pi \Delta y m \qquad \text{(Eq. 8)}$$

This uncertainty produces an uncertainty $\delta\theta$ in the scattering angle given by

$$\delta\theta \cong \Delta v_y / v_o \geq h/4\pi m v_o \Delta y \qquad \text{(Eq. 9)}$$

where v_o is the initial speed of the incident particle. Using Eq. (6), this may be written

$$\delta\theta \geq \lambda/4\pi\Delta y \qquad \text{(Eq. 10)}$$

Unless the scattering angle is much larger than $\delta\Theta$, quantum mechanics must be used to describe the collision even though the condition of Eq. (2) is met. For the example of He - Cu scattering at 1500 eV, Δy may be taken to be R = 10^{-12} m yielding a value for $\delta\theta$ of 0.03 radian, or less than 1.7°. The scattering angles used in ISS are typically 90° or larger, so this condition is met easily.
[Exercise 2] [Prerequisite Question 2]

C. Thermal Effects and Binary Collision Approximation

The foregoing considerations establish the validity of classical mechanics for the description of the ion-surface atom collision dynamics. The description is further simplified by two approximations: (1) that the thermal motion of the target atom can be ignored and (2) that the deflection of the probe ion is due to a binary collision; i.e. that the collision between the probe ion and surface atom is unaffected by the presence of neighboring atoms in the solid.

(1) Despite its thermal energy, the target atom may be assumed to be at rest for the following reasons. At 25°C, the energy of vibrational motion of an atom in a solid is only about 0.025 eV compared with typical incident ion energies of 1-2 keV. The amplitude of the vibrational motion is only a small fraction of the interatomic spacing and the period of vibration, about 10^{-13} sec., is long compared with collision times on the order of 10^{-15} sec.
[Exercise 3]

(2) The binary collision assumption is justified if, at the end of the ion-atom interaction, the kinetic energy of the recoiling surface atom is large compared with the change in its potential energy relative to its neighbors. Under these circumstances, the forces between the target atom and its neighbors cannot have affected the ion-atom collision significantly.

Returning again to the example of He - Cu scattering, numerical integration of the equations of motion for a head-on (worst-case) collision at 1500 eV shows the Cu atom to

move about 10^{-11} m while its kinetic energy reaches a final value of 260 eV. Moving 10^{-11} m closer to another copper atom involves a change in potential energy of only about 0.032 eV, and so the binary collision assumption clearly holds for this case. If the probe ion is changed from ^{3}He to ^{20}Ne, the ratio of kinetic to potential energy is decreased from about 8000 to about 1000, an amount still sufficient to justify the binary collision assumption.

[Exercise 4] [Prerequisite Question 3] [Prerequisite Question 4]

D. Relation Between Scattered Ion Energy and Target Mass

With the validity of classical mechanics and the above approximations established, the mass M_s of a surface atom may be deduced from measured quantities E_o, E, M_i and θ as follows. It is convenient to work with the momenta of the incident and deflected ion ($\vec{p_o}$ and $\vec{p}$, respectively) and of the recoiling particle ($\vec{p_s}$). The momentum conservation law requires that

$$\vec{p_o} = \vec{p} + \vec{p_s} \qquad \text{(Eq. 11)}$$

In Figure 3, $\vec{p_o}$ is shown graphically as the vector sum of $\vec{p}$ + $\vec{p_s}$; the scattering angle θ between the initial and final directions of the ion motion is also shown. The energy conservation law,

$$E_o = E + E_r$$

may be rewritten in terms of the momenta as

$$\frac{p_o^2}{2M_i} = \frac{p^2}{2M_i} + \frac{p_s^2}{2M_s} \qquad \text{or} \qquad \text{(Eq. 12)}$$

$$\frac{M_i}{M_s} p_s^2 = p_o^2 - p^2 \qquad \text{(Eq. 13)}$$

Applying the law of cosines to Figure 3,

$$p_s^2 = p_o^2 + p^2 - 2p_o\, p \cos\theta \qquad \text{(Eq. 14)}$$

and dividing Eq. (14) by Eq. (13) yields

$$\frac{M_S}{M_1} = \frac{p_o^2 + p^2 - 2pp_o \cos\theta}{p_o^2 - p^2} \qquad \text{(Eq. 15)}$$

Dividing by p_o^2 and noting that $p^2/p_o^2 = E/E_o$,

$$\frac{M_S}{M_i} = \frac{1 + E/E_o - 2\sqrt{E/E_o}\cos\theta}{1 - E/E_o} \qquad \text{(Eq. 16)}$$

and the surface atom mass M_S is expressed in terms of measured quantities. It is interesting that separate values of E and E_o are not needed but only their ratio.

In practice, surface atom masses are not calculated from Eq. (16). Instead tables of E/E_o vs. the masses M_S of the elements are computed and tabulated for each probe ion mass from the equation,

$$E/E_o = (1+\alpha)^{-2}\,[\cos\theta + (\alpha^2 - \sin^2\theta)^{1/2}]^2 \qquad \text{(Eq. 17)}$$

which follows from Eq. (16) when $\alpha = M_S/M_i \geq 1$. For commercial instruments, θ is fixed by the geometry of the equipment. A peak in the I vs. E spectrum is then associated with the mass M_S by looking at an appropriate table for the value of M_S corresponding to the E/E_o of the peak.
[Exercise 5] [Prerequisite Question 5]

E. Factors Which Affect the Scattered and Ion Yield

The considerations of the last section show how ISS can be used to deduce the elemental surface composition from the identified masses. It would clearly be valuable if, in addition to knowing an element is present, it were possible to deduce the amount of the species on the surface. Such quantitative information would be available if the heights of the peaks in the I vs. E spectra were related simply to the fraction of the surface covered by each detected element. Unfortunately, the relationship is not simple, and truly quantitative ISS requires a better understanding of the factors that affect the scattered ion yield.

The current I of ions resulting from the scattering of an ion beam by surface atoms of mass M_i can be expressed by

$$I_i = I_o\,(N_i - \Sigma\beta_{ij}\,N_j)\,P_i\,\Delta A_i \qquad \text{(Eq. 18)}$$

where I_o is the incident beam current, N_i is the number of scattering centers (of mass M_i) per unit area, β_{ij} is the fraction by which the targets of mass M_i are shadowed by

the surface species (including M_i) which has an areal density N_j, and P_i is the probability that the incident ion will not be neutralized in a collision with an atom of mass M_i. Now, ΔA_i may be described as follows. Each atom of mass M_i presents a more or less circular area to the incoming probe ions. ΔA_i is the part of that area which must be hit by a probe ion in order for the atom to be deflected toward the detector which measures I_i. The quantity ΔA_i obviously depends both on the ion-atom forces and on the size and location of the detector. These effects can be separated by writing

$$\Delta A_i = (d\sigma_i(\theta)/d\Omega)\Delta\Omega \qquad \text{(Eq. 19)}$$

Here $d\sigma_i(\theta)$ can be thought of as the infinitesimal area of an annulus centered on the target atom of mass M_i. Its radius is such that an ion passing through the annulus will be deflected by an angle near θ into an infinitesimal cone-shaped solid angle $d\Omega$. The ratio $d\sigma_i(\theta)/d\Omega$, which is called the differential cross-section for scattering at angle θ, depends only on the collision speed and the interatomic force. $\Delta\Omega$ is the effective solid angle of acceptance of the detector.

If a surface contains, for example, four species, a quantitative analysis requires that the four quantities N_i be deduced from a set of four equations of the form of Eq. (18) in terms of I_o, $\Delta\Omega$, and the four measured currents I_i.

Of the remaining terms in the equation, the cross-section $d\sigma_i(\theta)/d\Omega$ is the least troublesome. Reasonable calculations can be made of the cross-section for various ion-atom pairs. Figure 4 shows how this quantity varies with incident ion energy for He scattering from several different target atoms.

The shielding factors β_{ij} offer much more trouble since they depend on how each species is coordinated with the others and its location on the surface. In general the shielding factors will depend on the temperature, crystal face exposed, and the coverage of each species. Systematic studies of single crystal samples, oriented with respect to the incident beam direction and with controlled coverage of known species, will furnish important information about the shielding factors; unfortunately these data will be difficult to interpret until the last factor, P_i, is understood.

Whereas the motion of the colliding ion can be analyzed classically, the interactions of its electron shell with that of the target atom and with the electronic structure of the solid target are purely quantum mechanical problems. Current theoretical understanding

of these processes can explain the high probability with which the probe ion is found to be neutralized in terms of interactions between the electronic band structure of the solid and the electronic energy levels of the probe ion. The generally peaked shape of the scattered ion yield versus probe ion energy can be explained in terms of the competition between scattering cross-section, which falls with increasing energy, and the probability that the ion will escape neutralization, which rises with increasing energy (see Figure 5a).

Recent work which treats the colliding ion-atom pair as a temporary molecular ion provides a qualitative explanation of an interesting oscillatory structure that appears in the I vs. E_o curves for some systems (see Figure 5b). However, a theoretical formulation which satisfactorily combines the ion-atom and ion-crystal descriptions of neutralization has not yet appeared.

V. APPARATUS

The essential needs for ion scattering spectroscopy are a vacuum chamber, a sample holder, an ion gun, and an energy analyzer. The block diagram in Figure 6 shows the relationship among these components and some other required capabilities.

A. Vacuum Chamber and Sample Holder

Vacuum is required to permit the ions to traverse long trajectories without a significant number of collisions with gas molecules. The vacuum chamber must also provide a base pressure and residual gas background that is compatible with the samples to be investigated. Thus, the base pressure may range from 10^{-5} to 10^{-8} Pa for a UHV system of stainless steel construction. Baking in excess of 150°C is required if pressures below 10^{-7} Pa are to be reached.

Probe gases may be supplied to the ion gun by backfilling the chamber from an attached gas handling system. Some ion guns have a separately designed chamber which permits pressure differences of 1000:1 to exist between the sample and the ion gun. This is especially important for long experiments where gases may desorb from the vacuum walls, contaminate the probe gas, and react with the sample under investigation. A residual gas analyzer is frequently added to ISS systems to detect unwanted impurities

which may contaminate the probe gas from desorption and/or outgassing processes within the vacuum chamber.
[Exercise 6]

The sample holder may also have heating and cooling capabilities in addition to its obvious use. In some designs, the sample holder serves as a conducting path for measuring the ion beam current. The design should be appropriate for the investigations desired. In some cases, an assembly for loading several samples for sequential investigation is sufficient whereas in other cases rotation to change the scattering angle and azimuthal motion to change the alignment of a single crystal target are desired. Any material that is vacuum worthy can serve as a suitable sample.

B. Ion Source and Ion Beam

Ions are produced in a source by electron bombardment of a gas, usually He, Ne, or Ar, at pressures within an order of magnitude of 7×10^{-3} Pa. With the source held at the desired accelerating potential (~0.3 to 3 keV), ions are drawn from it by a negatively biased electrode. An ion beam is formed by an ion focusing lens system.

Important properties of the ion gun include producing a beam with an energy spread of only a few eV, a current in the range of 1 to 300 nA, and an angular divergence not greater than $\pm 1°$. The beam typically has a Gaussian shape in the ion number density with a Full Width at Half Maximum (FWHM) ranging from 0.1 to 3 mm, depending on the focusing voltages. The beam current must be stable so that repetitive scans of E/E_o from 0 to 1 will be responding to the same integrated projectile ion flux in ions/cm^2.

Correct measurement of the current can be made by applying a positive potential of about 25 volts to the target to suppress the effects of secondary electron emission, which may increase an uncorrected measured current by a factor of two or three. If, for example, each positive ion ejected one electron from the target on impact, a current twice as large as the beam current would be measured. Alternatively, the ion current may be measured by introducing a Faraday cup in place of the sample.

For most applications, only one type of singly charged ion species is desired in the beam;

e.g. ^{3}He, ^{4}He, ^{20}Ne or ^{40}Ar. Velocity filters, mass separators, differentially pumped sources, and gas exchange are techniques used to maintain probe gas purity. [Prerequisite Question 6]

C. Energy Analyzer

The energy of the scattered ions is measured by using an electrostatic analyzer, either of the sector-type or cylindrical mirror (CMA) type, to allow ions of specific energies to reach a channel electron multiplier detector (CEM). In the CMA, the ions are normally incident onto the sample, are scattered into an acceptance area of two concentric cones, and are focused onto the CEM by the electric field between two concentric cylinders. In the sector-type of electrostatic analyzer, the acceptance area is only a small arc of the acceptance area of the concentric cones and curved parallel plates are used, instead of concentric cylinders, to focus the ions onto the CEM. For most instruments, the scattering angle θ is fixed, but in custom-made spectrometers it may be varied. The voltage between the analyzer plates is ramped or stepped so that ions with successively higher energies are passed to the CEM. The pulses from the ions incident on the CEM are transmitted to a pre-amplifier, amplified, and sorted by a pulse height analyzer. The output of the pulse height analyzer is delivered to a ratemeter for the generation of an analog output which finally is input to an x-y plotter, a time base strip chart recorder, or computerized data acquisition system.

An ISS spectrum is obtained by simultaneously ramping the analyzer plate voltage and recording the output signal from the ratemeter. It consists of a series of peaks in the scattered ion current which occur at values of E/E_0 determined from Eq. (17) by substituting for M_s the masses of the surface atoms. In practice, the peak locations in E/E_0 are computed and tabulated for all elements and probe gases before the experiment, which reduces the analysis to searching the lists for the atomic masses that correspond to the E/E_0 peaks for the probe gas used [see text near Eq. (17)].

VI. TYPICAL SPECTRA

A typical ISS spectrum obtained from a treated polyvinylchloride film is shown in Figure 7. The peaks correspond to C, N, O, F, Na, Si, P (shoulder), Cl, Ti, and Sn. This is typical of hundreds of published spectra. The main feature of ISS spectra is that only one

peak appears for each element, or isotope of each element, as predicted from Eq. (17). Ten elements will yield ten peaks (Figure 7), which is considerably simpler than other widely used methods of surface analysis, notably, SIMS, AES and XPS. Masses of atoms (ions) may be detected on solid surfaces for samples that are conductors, semiconductors, and insulators. Qualitatively, the current detection sensitivity is 0.01 to 0.001 monolayers for the light elements and 0.0001 to 0.00001 monolayers for heavier elements, which have larger cross-sections. Other major advantages of ISS, which include monolayer sensitivity, surface structural information, isotope sensitivity, depth profiling, and chemical information, are discussed briefly below.

A. Monolayer Sensitivity

The detected signal results primarily, and possibly only, from atoms in the outer monolayer of atoms. Ions that penetrate into the second or deeper layers have such a high probability of being neutralized that the combination of an ion experiencing a single binary elastic collision (SBEC) and <u>not</u> being neutralized apparently provides an ion yield from inner layers below current detection limits. The monolayer sensitivity is illustrated by Figure 8, which shows different peak heights for a ZnTe single crystal cut to expose primarily Zn or Te ions. The monolayer sensitivity of ISS is in marked contrast to AES, where significant signal strength originates from 2 to 10 layers deep, depending on the solid.

B. Structural Information

ISS can provide important information about the structure or arrangement of two or more elements on ordered (e.g. single crystal) substrates. The location of S on Ni(100) and on Si(111) and of O on Ag(110), Ni(100), Ni(110), W, and Pb are among the recent examples cited in which shadowing of the projectile ion beam was used. Spectra showing this are presented in Figure 9 for oxygen ions on (110) silver. When the ion beam is directed toward the surface and at large angles to the normal, adsorbed atoms held deeply between two silver atoms are not detected (Curve 1); the oxygen ions are shielded from the beam by silver atoms. Rotation of the crystal by 90°, however, exposes them to the ion beam and the oxygen <u>is</u> detected (Curve 2).

C. Isotope Detection

ISS can be used to detect isotopes of the same element as reported recently for ^{16}O and ^{18}O in copper oxide films (Figure 10). The sensitivity of ISS to different isotopic masses provides a significant new dimension to ISS studies of catalytic reaction mechanisms, corrosion mechanisms, self-diffusion processes, adsorption-desorption phenomena, or any surface reaction where there is exchange of the same atomic species. Furthermore, it has been shown that quantitative analysis for a particular species in a well-characterized system can be made from analysis of the peak height intensity, as expected from Eq. (18) where I^+ is $\sim N_i$ and when all other factors are constant.

D. Depth Profile

The ion beam will gradually etch through a thin film to reach a solid-solid interface. As an example, Figure 11 shows a spectrum following etching through 44 nm of a copper oxide grown on a sodium chloride single crystal. All four elements are detected because the deepest part of the crater penetrates into the NaCl while the edges of the crater still yield signals from copper and oxygen.

E. Chemical Information

ISS can provide information about the influence of different chemical environments on the detected signal for the elements engaging in quasi-resonant transfer processes. Specific examples for some of the elements, such as Ga, Ge, As, In, Sn, Pb, and Bi that produce yield curves of the type shown by the solid line in Figure 5(b), are summarized in a recent chapter by Rusch and Erikson. Advanced students may want to tackle this excellent review chapter.

F. Resolution

Although an ISS spectrum is simple, it is unfortunate that the peaks are broad and that resolution between neighboring elements in the periodic table is poor. The curves in Figure 12 show calculated E/E_o ratios for different atomic masses when using ^3He, ^4He, ^{20}Ne, and ^{40}Ar probe ions. Inspection of the ^3He curve shows that all masses in the periodic table above 28 (silicon) will appear between E/E_o of 0.7 and about 0.96. With

peak widths typically between 0.015 and 0.04 in E/E_o at FWHM, clearly peak overlap will result in poor resolution. The curves for ^{20}Ne and ^{40}Ar show improved resolution because of the smaller slope, but they also show that masses below 23 (for Ne) and 46 (for Ar) are not detectable for the heavier probe gases. Figure 13 illustrates the crowding of peaks when ^{4}He is scattered from a Au-Mo-Ni surface and their clean separation when ^{20}Ne is used. Consulting a set of curves to determine the possibility of peak interference should be a prerequisite for considering the potential value of using ISS on a sample of known composition.

G. Other Factors

Noble ions must be used for ISS because reactive gases do not produce symmetrical peaks. For example, Figure 14 shows scattering of $^{3}He^{+}$ and $^{1}H^{+}$ from a clean Pd surface. It should be obvious that additional peaks below the principal peak would be difficult to identify. Furthermore, the maximum of the hydrogen peak does not occur at the position for a SBEC.

A good vacuum is required ($\sim 10^{-6}$ Pa) and, where reactive surfaces are studied, the vacuum should be $\sim 10^{-8}$ Pa. The surface under investigation will be damaged by the bombardment from the projectile ions. Even though reduced bombardment energies ($\sim$300-700 eV) and low current densities (0.4 to 40 $\mu A/cm^2$) may be employed, sputtering of the outer monolayer is unavoidable.

If an insulating sample is studied, positive charge will accumulate on the surface, producing displacement of the peaks from the position expected for a SBEC. The positive charge buildup can be eliminated by flooding the surface with thermal electrons by means of a charge neutralization filament.

A considerable amount of additional information is available in ISS spectra. The yield curve of a typical ISS energy loss spectrum also contains low energy (sputtering) peaks, multiple scattering peaks, peaks from doubly ionized particles, and tailing on the low energy side of a SBEC ISS peak. Many scattered ion yield curves are rich in fine features that can be used to distinguish between elements with unresolvable ISS peaks or to obtain chemical information, but these details are beyond the scope of this module.

VII. SUMMARY

The interpretation of ISS spectra is simple because of the agreement with the single binary elastic collision model. Qualitative identification of elements in the surface monolayer is routinely possible to 10^{-3} to 10^{-5} of a monolayer. Quantitative analysis is possible when careful procedures are followed, but more data are needed about neutralization probabilities and scattering cross-sections to expand this area of feasibility. In comparison with other surface techniques, ISS offers outstanding advantages in monolayer sensitivity, structural analysis, and isotope sensitivity in addition to providing chemical information for elements undergoing quasi-resonant charge exchange neutralization processes. Its chief limitations result from poor resolution at large masses, where its detection sensitivity is the best, and from unavoidable damage to samples.

VIII. SUPPLEMENTARY MEDIA

A movie comparing ion scattering with billiards was produced and is available from H. Brongersma, Philips, Eindhoven, The Netherlands. A movie on sputtering can be obtained from Prof. N. Winograd, Penn State, University Park, PA 16802.

IX. FURTHER READING

Books

1. N. F. Mott and H. S. W. Massey, The Theory of Atomic Collisions, Clarendon Press, Oxford, 1965.

2. Manfred Kaminsky, Atomic and Ionic Impact Phenomena on Metal Surfaces, Academic Press, New York, 1965.

3. G. Carter and J. S. Colligon, Ion Bombardment of Solids, American Elsevier Publishing Co., New York, 1968.

Review Chapters in Books or Journals

1. D. P. Smith, "Analysis of Surface Composition with Low-Energy Backscattered Ions,"

Surface Sci. 25 (1971) pp. 171-191.

2. H. H. Brongersma and P. M. Mul, "Analysis of the Outermost Atomic Layer of a Surface by Low-Energy Ion Scattering," Surface Sci. 35 (1973) pp. 393-412.

3. T. M. Buck, "Low-Energy Ion Scattering Spectrometry," in Methods of Surface Analysis, A. W. Czanderna (ed.), (Elsevier, Amsterdam, 1975) pp. 75-102.

4. R. E. Honig, "Surface and Thin Film Analysis of Semiconductor Materials," Thin Solid Films 31 (1976) pp. 89-122.

5. E. Taglauer and W. Heiland, "Surface Analysis with Low Energy Ion Scattering," Appl. Phys. 9 (1976) pp. 261-275.

6. G. C. Nelson, "The Analysis of Solid Surfaces by Low Energy Ion Scattering Spectroscopy," J. Colloid Interface Sci. 55 (1976) pp. 289-296.

7. T. Rusch and R. L. Erickson, "Oscillatory Scattered Ion Yields in Low Energy Ion-Surface Scattering," in Inelastic Ion Surface Collisions, N. H. Tolk, J. C. Tully, W. Heiland and C. W. White (eds.), (Academic Press, N.Y. 1977) pp. 73-104.

Recent Journal Articles

1. H. H. Brongersma and T. M. Buck, Surface Sci., 53, 649 (1975). (Surface Enrichment in Cu-Ni alloys).

2. W. Heiland and E. Taglauer, Surface Sci., 68, 96 (1977). (Surface Structure of Adsorbed Species).

3. A. W. Czanderna, A. C. Miller, H. H. G. Jellinek and H. Kachi, "Ion Scattering Analysis of Copper Films Oxidized in ^{18}O," J. Vac. Sci. Technol. 14 (1977) pp. 227-230; "Isotope Masses by ISS," Industrial Research (January 1978) pp. 62-64. (Isotopic Labeling).

4. H. F. Helbig, P. J. Adelmann, A. C. Miller, and A. W. Czanderna, "Displacement of

Ion Scattering Peaks from Positions Predicted by Binary Scattering," Nuclear Instr. Methods 149 (1978) 581. (Other Factors, Charging Effects).

5. W. L. Baun, "Fine Features in Ion Scattering Spectra (ISS)," Appl. Surface Sci. 1 (1978) 126. (Other Factors).

Exercise 1

For 1500 eV helium-3, show that the de Broglie wavelength is 4.27×10^{-13} m and that $\Delta V/V$ is 0.4.

Exercise 2

Verify $\delta\theta = 0.03$ radian for 1500 eV helium 3 using Eq. (10).

Exercise 3

Estimate the collision time for 500, 1000 and 2000 eV, ^{4}He and ^{20}Ne with an atom in a solid surface. Assume the "collision" occurs over a path of 10^{-10} m at the constant speed of approach to the surface. How would the actual path and speed of the ion change your calculated collision time and why?

Exercise 4

Calculate the potential energy of two copper atoms at an equilibrium separation of 3×10^{-10} m. Calculate the change in repulsive potential energy if the atom moves 10^{-11} m (a) closer to, (b) away from, its nearest neighbor. Assume the potential energy is given by $V = (Z_1 Z_2/r)e^{-r/a}$, where a is about 10^{-11} m. Compare this change in PE with that of the recoil kinetic energy of the copper atom in the last paragraph of Section IVC.

Exercise 5

(a) Show Eq. (17) reduces to $E/E_o = (M_s - M_i)(M_s + M_i)$ for a 90° scattering angle.

(b) For 90° ^{4}He scattering, peaks occur at E/E_o of 0.6 and 0.88. What elements are present on the surface?

Exercise 6

The collision frequency of a gas molecule with the container walls is $\nu \cong P/(2\pi m\, kT)^{1/2}$ where P is the pressure, m is the mass of the gas molecule, k is the Boltzmann constant, and T is the temperature in K. Show that at 1.3×10^{-4} Pa, $\nu = 3.6 \times 10^{18}$ collisions/m^2-s for oxygen (amu = 32) at 300K. If every molecule that hits a clean surface sticks, how long will it take to completely contaminate a 1-cm^2 sample?

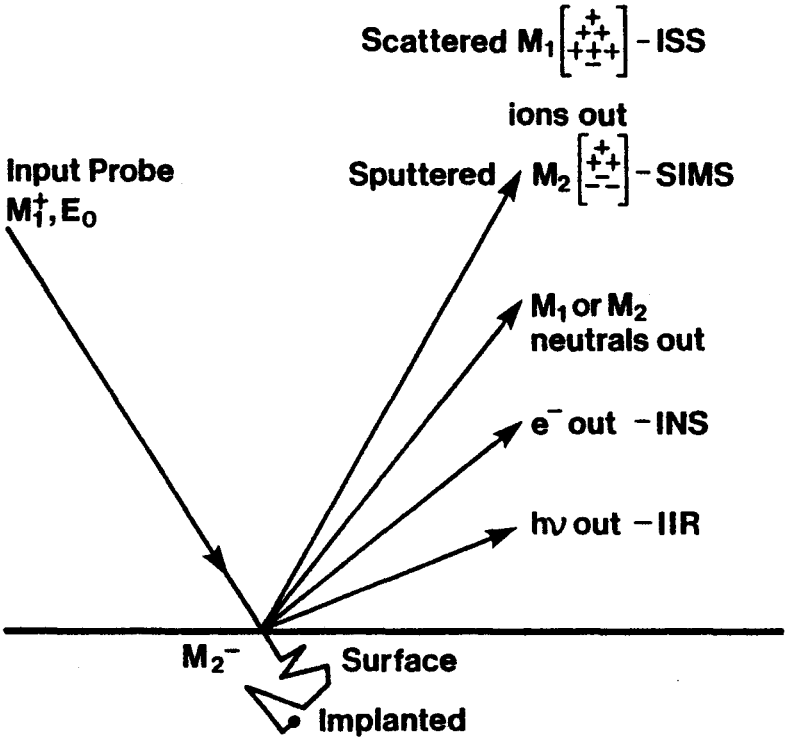

Fig. 1 Schematic of techniques involving ions as the exciting probe. ISS, ion scattering spectrometry; SIMS, secondary ion mass spectrometry; INS, ion neutralization spectroscopy; IIR, ion induced radiation; PIX, proton-induced X-rays.

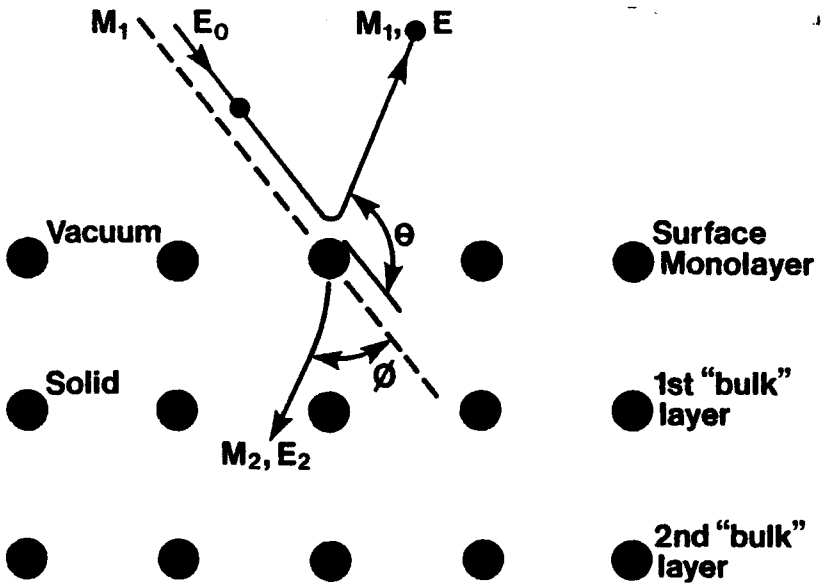

Fig. 2 Schematic representation of the scattering of a projectile ion from a surface atom and the recoil of the surface atom M_S with the energy E_S.

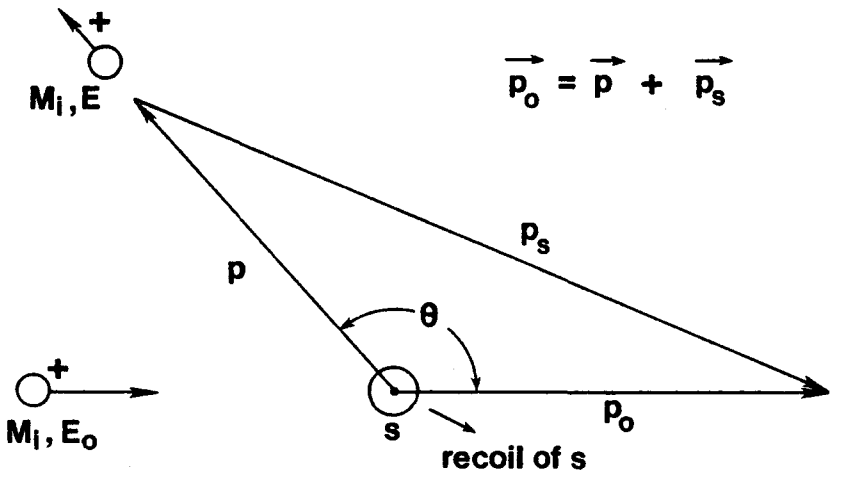

Fig. 3 Diagram showing that the vector sum of momenta after the collision equals the initial momentum p_O.

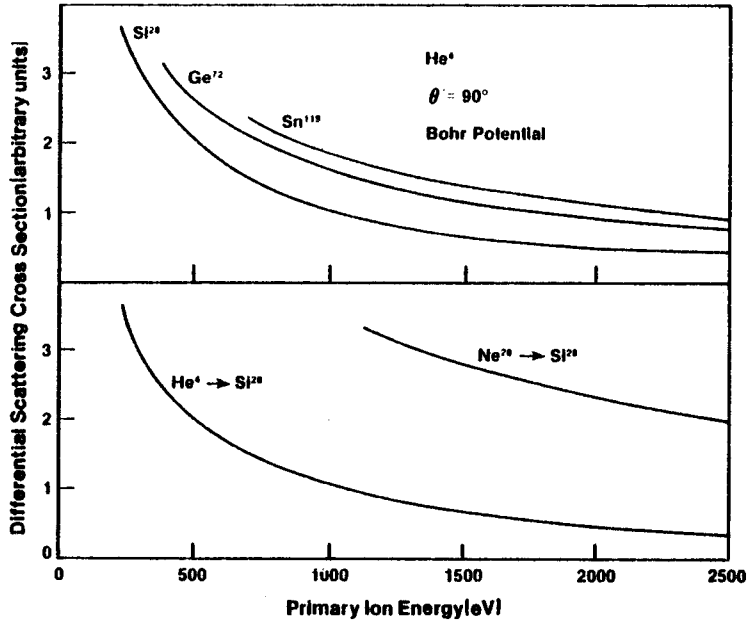

Fig. 4 Differential scattering cross-section as a function of primary ion energy calculated using the Bohr potential.

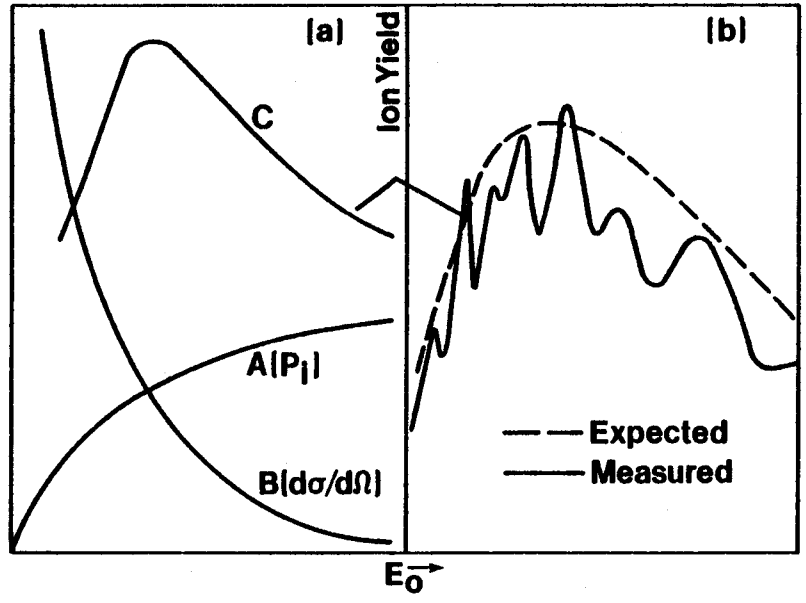

Fig. 5 The ion yield as a function of incident ion energy for two different classes of elements. Curve C in (a) shows the expected and observed behavior for "normal" elements. The solid line in (b) shows an oscillatory structure.

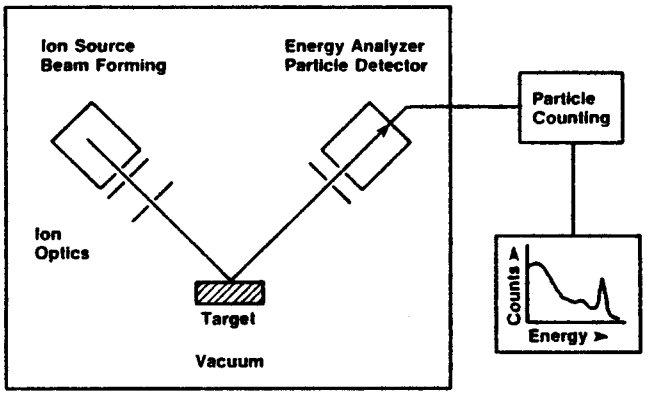

Fig. 6 Scheme for an ion scattering experiment.

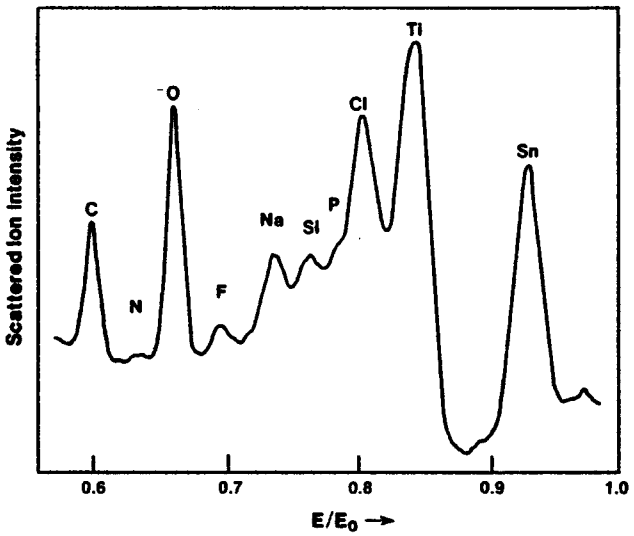

Fig. 7 ISS spectrum for a treated polyvinylchloride (PVC) film using helium-4 at 1.5 keV and 60 nA.

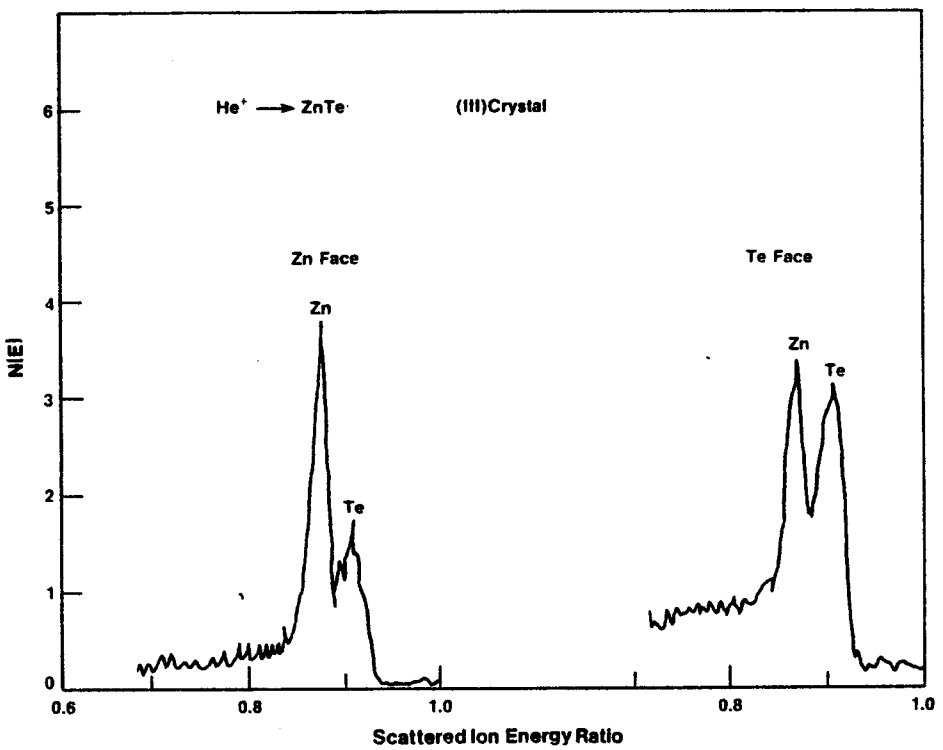

Fig. 8 ISS spectra from different faces of a ZnTe single crystal show sensitivity to the surface monolayer.

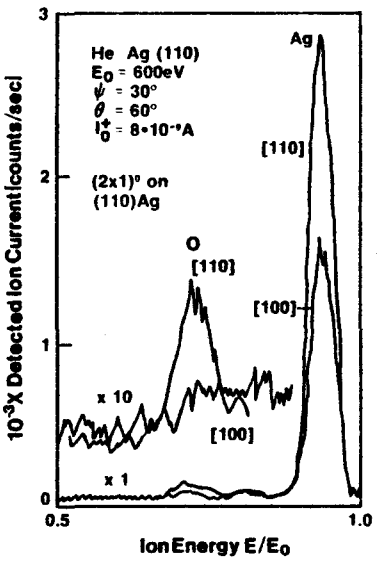

Fig. 9 ISS spectra from a silver single crystal covered with half a monolayer of oxygen, which forms a well-defined surface monolayer of "Ag_2O". Curve 1, (100); Curve 2, (110); note the attenuation factor for the silver peak compared with that for oxygen.

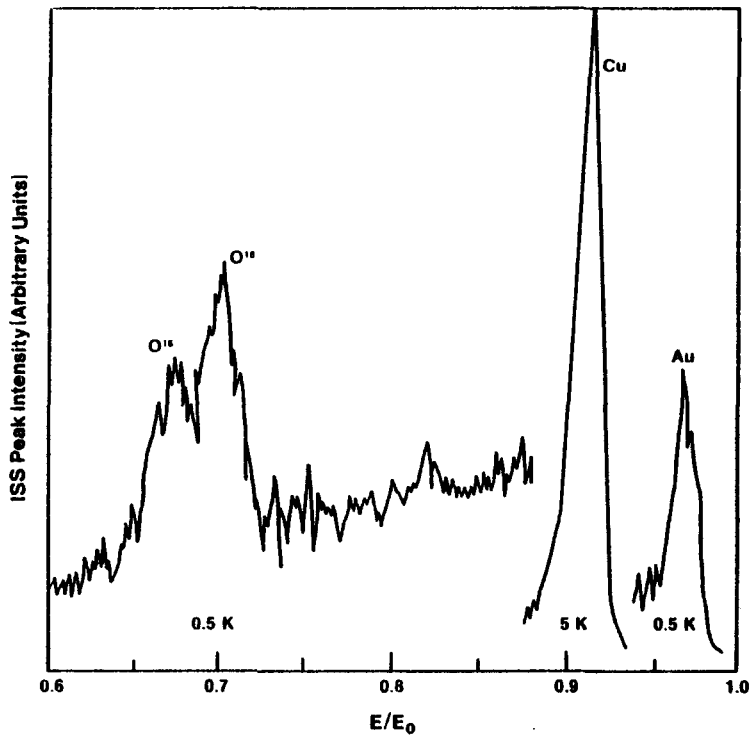

Fig. 10 ISS spectrum for an isotopically labeled copper oxide film grown on gold after ion etching to the oxide/gold interface.

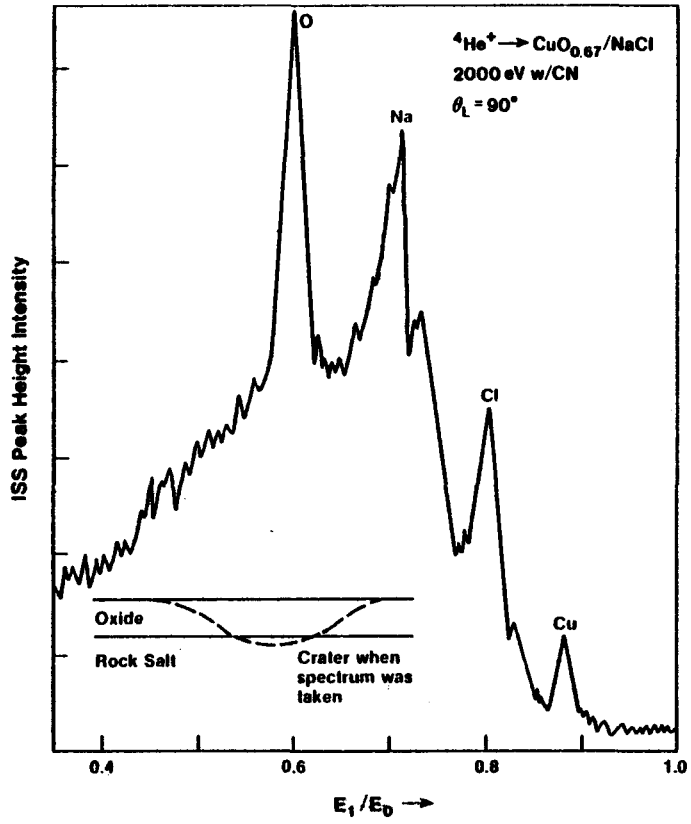

Fig. 11 ISS spectrum for a copper oxide film formed on rock salt in oxygen-16 after ion etching to the oxide/NaCl interface (inset).

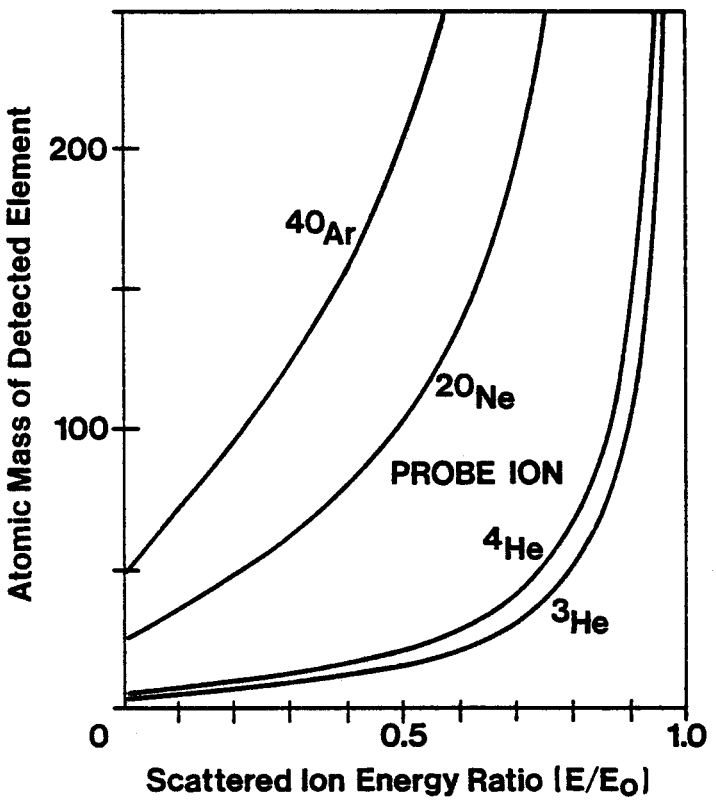

Fig. 12 The scattered ion energy ratio for elemental masses using different inert gas probe ions and a fixed scattering angle of 138°.

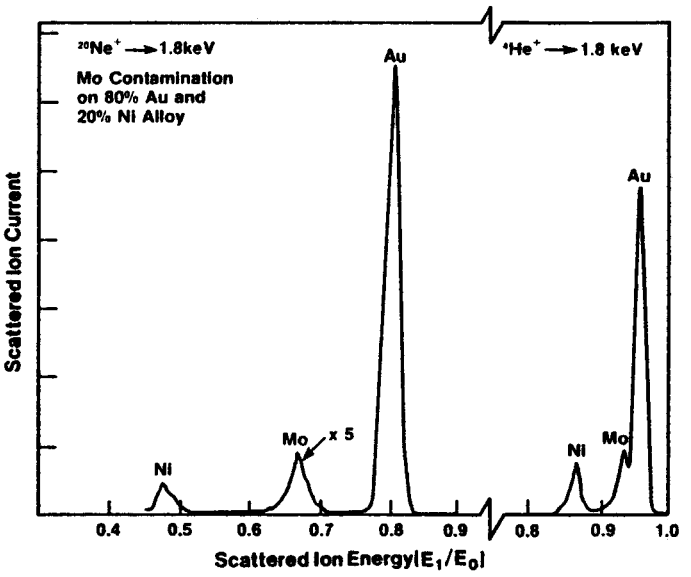

Fig. 13 ISS spectra for helium-4 and neon-20 scattered from a gold-nickel alloy with a molybdenum surface impurity. Note the improved mass resolution obtained with the heavier probe ion.

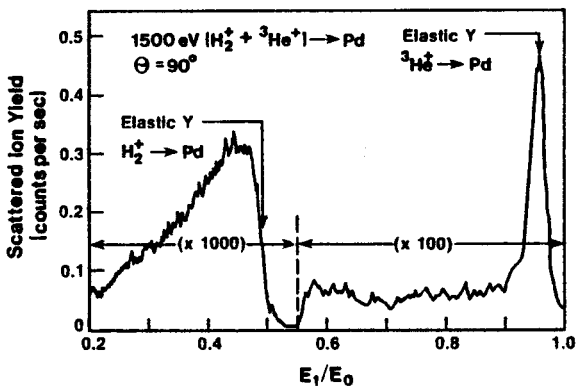

Fig. 14 ISS spectrum for a mixture of helium and hydrogen incident on palladium. The energies for a SBEC are indicated by the vertical arrows.

SERI

DISTRIBUTION LIST

No. of Copies	Distribution
1	Department of Energy: DOE, SERI Site Office Contracting Officer Attn: Charles M. Skinner
1	Chicago Operations Office Interim Program Division Attn: M. E. Jackson
1	Division of Solar Technology Office of Asst. Director for Administration Attn: R. H. Annan
1	Office of Asst. Secretary for Conservation & Solar Applications Attn: R. Scott
1	Office of Solar, Geothermal, Electric & Storage Programs Attn: Martin Adams
1	Division of Energy Technology Administration Attn: S. Hansen
1	Division of Distributed Solar Technology Office of the Director Attn: R. San Martin
1	Division of Central Solar Technology Office of the Director Attn: H. Coleman
1	Division of Energy Storage Systems, ETS Office of the Director Attn: G. Pezdirtz
1	Division of Planning & Energy Transfer, ETS Office of the Director Attn: Leslie Levine
1	Wind Energy Systems Attn: L. Divone